Analysis of Power Recycling Techniques for RF and Microwave Outphasing Power Amplifiers

Xuejun Zhang, Lawrence E. Larson, *Fellow, IEEE*, Peter M. Asbeck, *Fellow, IEEE*, and Robert A. Langridge, *Member, IEEE*

Abstract—A power recycling technique has been analyzed for efficiency-enhanced radio-frequency (RF) and microwave outphasing power amplifiers for mobile wireless communications. By use of a simple power recycling network, a considerable portion of the wasted power can be recovered back to the power supply, and the enhancement of the overall power efficiency can be achieved without sacrificing the high-linearity performance of the amplifier system. An analysis and calculations have been conducted to optimize the recycling network for the maximum power efficiency. The results predict a significant improvement on the overall power efficiency of the amplifier system for various modulations.

Index Terms—Linear amplification with nonlinear components (LINC), outphasing power amplifiers, radio-frequency (RF) linear power amplifiers.

I. INTRODUCTION

LINEAR modulations such as MPSK and MQAM are desired for mobile wireless communications because of their superior spectral efficiency, but they require linear power amplification at transmission. On the other hand, limited battery capacity imposes primary restrictions on the power consumption of the typical mobile handset, and even base station power amplifiers have limited dc power availability. In a typical transceiver architecture, it is typically the final power amplifier stage that constitutes these real challenges for the designer. Many linearization techniques have been proposed to improve the linearity of the power amplifiers while at the same time enhancing the power efficiency. The outphasing power amplifier is one of the promising techniques that can achieve high linearity and high power efficiency simultaneously. The "outphasing" concept dates back to the early 1930s and has been recently re-invigorated under the rubric of linear amplification with nonlinear components (LINC) [1]–[11]. The outphasing approach takes an envelope modulated bandpass waveform and resolves it into two outphased constant envelope signals, which are amplified

separately with two highly efficient nonlinear power amplifiers and then summed. This approach allows the power amplifiers to continuously operate at their peak power efficiency—potentially improving the power efficiency of the system, and yet the final output can be highly linear.

However, one of the disadvantages of this approach is the power loss inside the combining network, which compromises the overall power efficiency, e.g., when a conventional hybrid is used as the power combiner [8]. Alternative combining approaches improve the power efficiency by use of reactive combiners without the power termination [5]–[7]. These methods may suffer from the incomplete isolation between the two power amplifiers, i.e., the two power amplifiers "appear" to interfere with each other. As a result, a significant signal distortion can occur and the system linearity is degraded.

A power recycling technique was proposed in [10] as an attempt to enhance the power efficiency while maintaining sufficient isolation. This paper presents the detailed analysis of the power recycling scheme to optimize the recycling network for the maximum efficiency performance. The analysis begins with an analysis of a simple constant envelope waveform in order to gain insight. Then, linear modulated signals are discussed and the numerical results are presented.

II. POWER RECYCLING TECHNIQUE FOR OUTPHASING AMPLIFIERS

A complex representation of the band-limited source signal can be written as

$$s(t) = r(t)e^{j\theta(t)}, \qquad 0 \le r(t) \le r_{\max}. \tag{1}$$

This signal is split by the signal component separator (SCS) of the outphasing amplifier into two signals with modulated phase and constant amplitude

$$S_1(t) = s(t) - e(t) \tag{2a}$$
$$S_2(t) = s(t) + e(t) \tag{2b}$$

where the quadrature signal $e(t)$ is defined by

$$e(t) = js(t)\sqrt{\frac{r_{\max}^2}{r^2(t)} - 1}. \tag{3}$$

The two signals are then amplified individually and fed to the power combining network. With the combiner, the in-phase signal components add together and the out-of-phase signal components cancel out, therefore, the desired output is obtained.
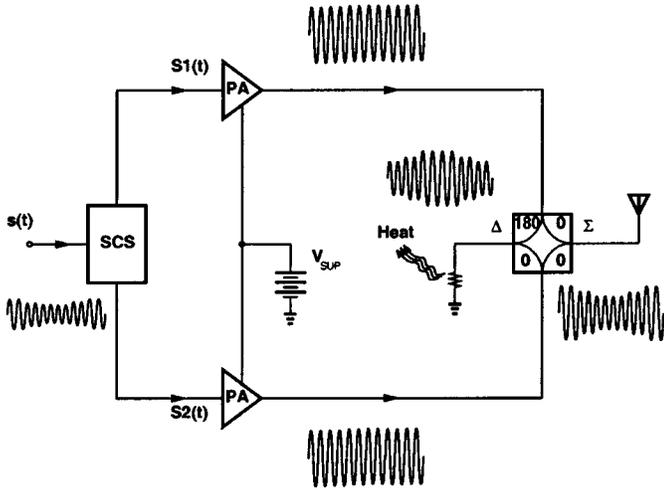
Fig. 1. Outphasing power amplifier with hybrid power combining.

An efficient power combining approach is necessary to preserve the high power efficiency of the system. The purely reactive combiner such as Chireix combining and the lossless "tee" combiner [6] are possible choices. However, this method suffers from a variation of the load impedance presented to the two power amplifiers, which in turn creates the signal distortion. The load variation, which results from the time varying phase offset between the two signal components, can be eliminated with a conventional hybrid combiner, as shown in Fig. 1. In the ideal case, the hybrid completely isolates the two power amplifiers and each amplifier "sees" a 50-Ω load. With the hybrid, the desired output signal is obtained on the summing port, while the quadrature signal is obtained on the difference port. Unfortunately, the latter portion of the power is consumed at the resistive load and turns into waste heat, which degrades the overall power efficiency. Since the instantaneous combining efficiency is the ratio of the desired output power to the total power delivered by the two power amplifiers, the average combining efficiency is easily calculated by [8]

$$\overline{\eta}_c = \int_0^1 \rho(r) r^2 \, dr \tag{4}$$

where r is the normalized output signal magnitude, and $\rho(r)$ is the probability density function of the modulation. The wasted power compromises the overall power efficiency, especially for high-level modulations, in which the signal experiences a wide range of variation of the power levels. For example, the overall power efficiency is 45% for $\pi/4$-DQPSK modulated signal with square-root raised cosine filtering of roll-off 0.35, and drops to 17% for 64-QAM modulated signal with the same filtering [8]. Note that the average combining efficiency is equivalent to the average-to-peak power ratio of the modulations.

The idea of the power recycling scheme is simple—replace the power-wasting resistive load by an RF-dc converter to recover as much of the wasted power as possible back to the power supply. The schematic diagram of an implementation of this scheme is illustrated in Fig. 2. A 180° hybrid combiner is configured as the power splitter to divide the wasted power into two 180° outphased portions. These two signals are then fed to a

high-speed Schottky diode pair through an impedance matching network. The Schottky diodes rectify the RF waves and the dc components are withdrawn to the power supply. The RF "choke" loops provide a dc return path for the circuit. The matching network is to be adjusted to optimize the system performance. As it turns out, the efficiency of the recycling network is highly dependent on the power supply voltage, the characteristics of the diodes as well as the power delivered to the recycling network.

III. THEORETICAL ANALYSIS FOR CONSTANT ENVELOPE WAVEFORM

The constant envelope waveform is examined first to identify the tradeoffs involved in the recycling network for the maximum performance. To simplify the analysis of Fig. 2, an ideal resistive model is assumed for the Schottky diode, i.e., a fixed "on-resistance" R_d in series with the built-in potential V_d, an infinite "off-resistance," and negligible shunt capacitance. All other components are assumed ideal. The analysis starts from the diode side. Since the 180° hybrid combiner is used as the power splitter, each diode conducts less than half time and operates 180° out-of-phase. The current through the upper diode is, thus, described by

$$I_d(t) = \begin{cases} \dfrac{V_{\mathrm{pk}} \cos \omega_c t - (V_{\mathrm{sup}} + V_d)}{R_d}, & \cos \omega_c t \geq \dfrac{V_{\mathrm{sup}} + V_d}{V_{\mathrm{pk}}} \\ 0, & \text{otherwise} \end{cases} \tag{5}$$

where V_{sup} is the power supply voltage, V_{pk} is the peak signal voltage applied to the diode, and ω_c is the carrier frequency of the signal. The diode conduction angle θ is given by

$$\cos \theta = \frac{V_{\mathrm{sup}} + V_d}{V_{\mathrm{pk}}}, \qquad 0 \leq \theta < \frac{\pi}{2}. \tag{6}$$

Note its symmetry with respect to the origin, the diode current can be expanded as the following Fourier series

$$I_d(t) = i_0 + \sum_{k=1}^{\infty} i_k \cos(k\omega_c t) \tag{7}$$

where i_k is the kth-order harmonic of the diode current. It can be shown that the fundamental components and all odd-order harmonic current of the two diodes are 180° out of phase, hence, cancel out; only the dc components and even-order harmonics are left. As we know that the RF "chokes" are usually embedded with the power amplifiers, hence, a large value shunt capacitor may be sufficient to short the harmonic currents to the ground, as shown in Fig. 2. The dc component of the diode current is given by

$$i_0 = \frac{1}{2\pi} \int_{-\theta}^{\theta} I_d(\phi) \, d\phi \tag{8a}$$

$$= \frac{V_{\mathrm{sup}} + V_d}{\pi R_d} (\tan \theta - \theta). \tag{8b}$$

The recycled portion of the power is, hence

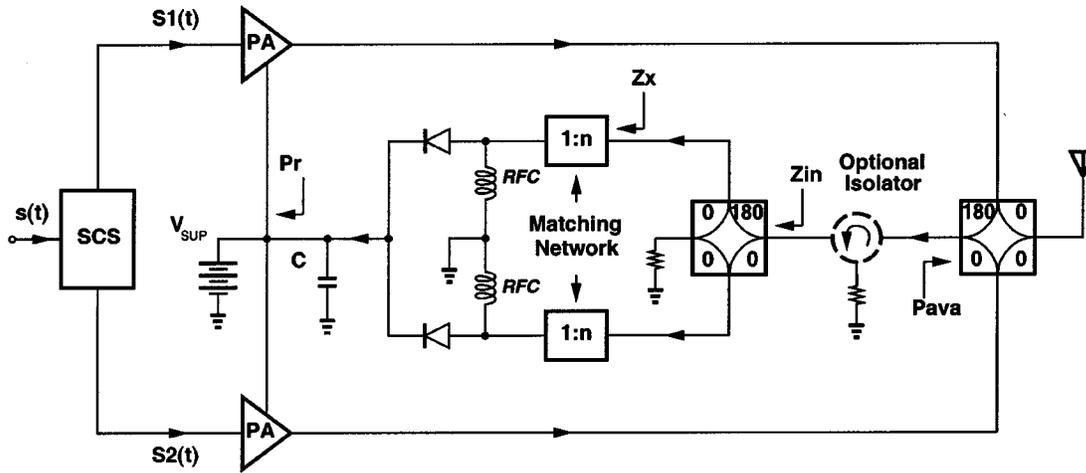$$P_r = 2i_0 V_{\mathrm{sup}}. \tag{9}$$

Fig. 2.   Outphasing power amplifier with the power recycling network.

The RF-dc power conversion is a strongly nonlinear process. In such a case, the large signal impedance of the device is usually estimated by the fundamental component of the voltage and current waveforms. The fundamental component of the diode current at ω_c is, thus

$$i_1 = \frac{1}{\pi} \int_{-\theta}^{\theta} I_d(\phi) \cos\phi \, d\phi \tag{10a}$$

$$= \frac{V_{\text{sup}} + V_d}{\pi R_d} (\theta \sec\theta - \sin\theta). \tag{10b}$$

The impedance matching network scales the diode voltage and current seen from the hybrid combiner. We assume an impedance transformation ratio of $n : 1$ from the hybrid side to the diode side. The hybrid can also be considered as an impedance transformer, and it can be shown that the input impedance of the recycling network is actually equal to Z_x—the impedance looking into the impedance matching network from the hybrid as shown in Fig. 2. So

$$Z_{\text{in}} = n^2 \frac{V_{\text{pk}}}{i_1} \tag{11a}$$

$$= \frac{\pi n^2 R_d}{\theta - \sin\theta \cos\theta}. \tag{11b}$$

The reflection coefficient of the recycling network is, thus

$$\Gamma_{\text{in}} = \frac{Z_{\text{in}} - Z_0}{Z_{\text{in}} + Z_0} \tag{12}$$

where Z_0 is the characteristic impedance and assumed as 50 Ω. The voltage standing-wave ratio (VSWR) is, according to the standard definition

$$\text{VSWR} = \frac{1 + |\Gamma_{\text{in}}|}{1 - |\Gamma_{\text{in}}|}. \tag{13}$$

The available power to the recycling network needs to be known in order to calculate the recycling efficiency. The input impedance of the recycling network varies with the diode conduction angle, which is in fact determined by the power delivered to the recycling network. In practice the situation is complicated by the coupling between the variation of the load impedance and the power delivered by the amplifiers. For example, a load impedance variation may drive a class-AB or class-B power amplifier into saturation or breakdown. A few power amplifiers that are sensitive to the load impedance and require careful tuning, like class-E amplifiers, may fail to work in this case. Furthermore, as stated previously, the load impedance variation introduces an incomplete isolation between the two power amplifiers even with the hybrid combiner. Because of the load line match of the power amplifiers, the wideband quadrature signal reflected from the difference port of the hybrid is reflected to the summing port, though the hybrid provides an additional 3-dB isolation. The signal mixes with the desired output signal and create the signal distortion. An isolator may be placed between the two hybrids to absorb the power reflected from the impedance matching network and eliminate this effect. In this case, looking from the hybrid combiner, the load is always matched to 50 Ω, while looking from the hybrid splitter, the isolator acts like an ideal voltage source V_s with an internal resistance of 50 Ω—the maximum power transfer theorem applies. Thus, the source voltage is

$$V_s = \sqrt{2}\, n V_{\text{pk}} + \sqrt{2}\, \frac{Z_0 i_1}{n} \tag{14}$$

where the scaling factor "n" results from the $1 : n$ impedance matching network and the $\sqrt{2}$ comes from the fact that the hybrid is a power addition device. The available power to the recycling network is then

$$P_{\text{ava}} = \frac{1}{8} \frac{V_s^2}{Z_0} \tag{15a}$$

$$= \frac{(V_{\text{sup}} + V_d)^2}{4 Z_0} \left[n \sec\theta + \frac{Z_0}{n \pi R_d} (\theta \sec\theta - \sin\theta) \right]^2. \tag{15b}$$

For a hybrid combiner with matched loads, the out-of-phase portion of power from power amplifiers—$e(t)$ in (2a) and (2b)—sum together in the difference port and the in-phase portion cancel out. Therefore, the available power to the recycling network corresponds to the portion of the quadrature
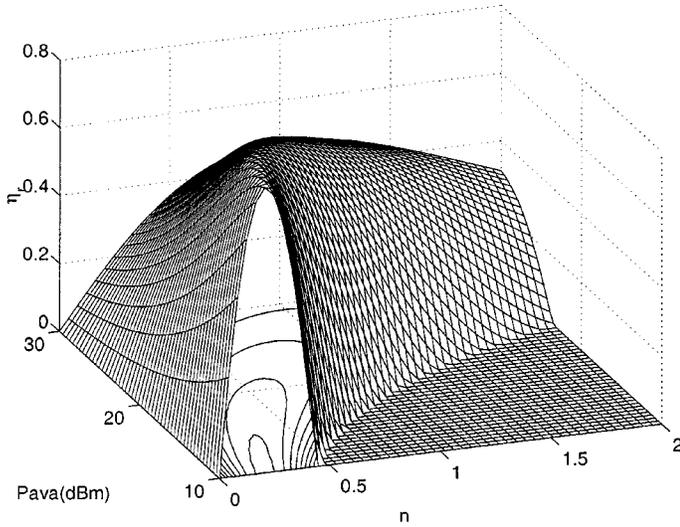
Fig. 3. Recycling efficiency as the function of "n" and the available power. $R_d = 10 \ \Omega$.

Fig. 4. VSWR as the function of "n" and the available power. $R_d = 10 \ \Omega$.

signal $e(t)$, and a simple relation exists between the available power and the transmitted power P_{out}

$$P_{\mathrm{ava}} = P_{\mathrm{max}} - P_{\mathrm{out}} \tag{16}$$

where P_{max} is the maximum transmitted power.

The recycling efficiency is defined as the ratio of the recycling power over the available power to the network

$$\eta_r = \frac{P_r}{P_{\mathrm{ava}}}. \tag{17}$$

Now that a portion of the previously wasted power ($\eta_r P_{\mathrm{ava}}$) has been recycled, the overall power efficiency with the recycling network is given by

$$\eta_o = \frac{\eta_h}{1 - (1 - \eta_h)\eta_r} \tag{18}$$

where η_h is the power efficiency without power recycling. The overall power efficiency is enhanced through the recycling network. The net improvement on efficiency becomes more evident as η_h decreases. In the ideal case with 100% recycling efficiency, the overall power efficiency becomes 100%.

Figs. 3 and 4 show three-dimensional plots of the calculated recycling efficiency η_r and VSWR as a function of the impedance transformation ratio "n" of the matching network and the available power "P_{ava}" to the recycling network, respectively. The following parameters were chosen for the computation: $V_{\mathrm{sup}} = 3$ V, $V_d = 0.4$ V, and $R_d = 10 \ \Omega$. The contour plots are also shown beneath the mesh plots. It is clear that there is a close relationship between the maximum recycling efficiency and the lowest VSWR. There are two different cases of particular interest—the constant power available to the recycling network case and the fixed impedance matching network case. For the former case, the maximum recycling efficiency can be found by differentiating (17) with respect to
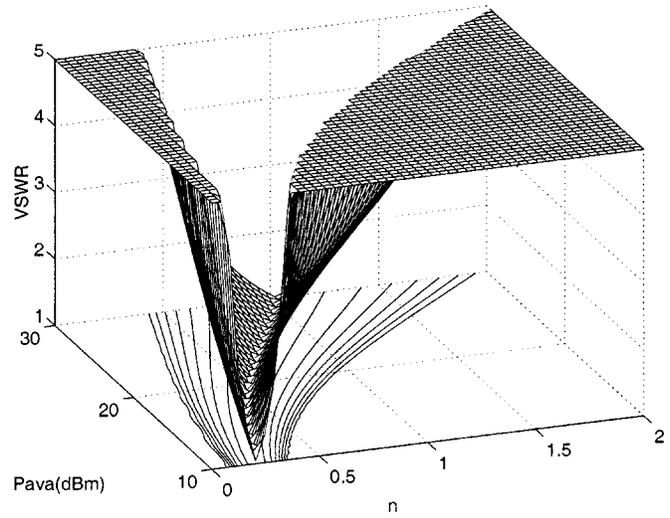
the impedance transformation ratio, with constant available power, i.e.

$$\frac{d\eta_r}{dn} = \frac{d\eta_r}{d\theta} \frac{d\theta}{dn}. \tag{19}$$

The derivative of the diode conduction angle with respect to the impedance transformation ratio $d\theta/dn$ can be found from (15), which is regarded as the implicit function of the "n" and the diode conduction angle θ, since P_{ava} is a constant. Finally, we get

$$\frac{d\eta_r}{dn} = -\frac{2V_{\mathrm{sup}}}{P_{\mathrm{ava}}} \sin\theta \frac{V_{\mathrm{pk}}(\theta) - \frac{Z_0}{n^2} i_1(\theta)}{n\pi R_d + \frac{Z_0}{n} (\theta + \sin\theta\cos\theta)}. \tag{20}$$

The maximum recycling efficiency occurs when the above expression is equal to zero, and that is equivalent to the following condition:

$$Z_0 = n^2 \frac{V_{\mathrm{pk}}}{i_1} \tag{21a}$$

$$= Z_{\mathrm{in}}. \tag{21b}$$

Equation (21) concludes that the optimum VSWR of the recycling network is equivalent to the optimum recycling efficiency as the available power to the recycling network is fixed. This conclusion also applies to the arbitrary diode model, as proved in the Appendix. From (15), (17), and (21) it can be shown that the maximum recycling efficiency as a function of the diode conduction angle is given by

$$\eta_{r,\mathrm{max}} = \frac{V_{\mathrm{sup}}}{V_{\mathrm{sup}} + V_d} \frac{4(\tan\theta - \theta)}{2\theta - \sin 2\theta} \cos^2\theta \tag{22a}$$

$$\approx \frac{4(\tan\theta - \theta)}{2\theta - \sin 2\theta} \cos^2\theta \tag{22b}$$

assuming $V_{\mathrm{sup}} \gg V_d$, which is a reasonable approximation in most practical applications. The diode conduction angle in the above expression, of course, corresponds to the case with the optimum impedance matching. A figure of merit which indicates the capability of the recycling network can be defined as the recycling factor, which determines the diode conduction angle
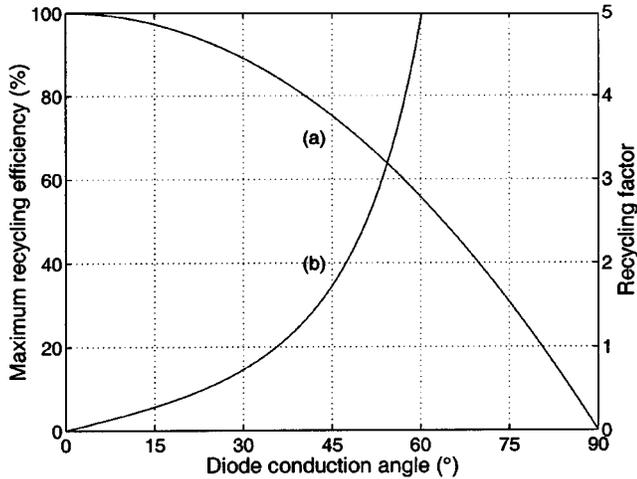
Fig. 5. (a) Maximum recycling efficiency. (b) Recycling factor as a function of the diode conduction angle.

Fig. 6. Maximum recycling efficiency as a function of the recycling factor.

under the optimum impedance matching

$$\epsilon_r = \frac{2\pi R_d P_{\mathrm{ava}}}{(V_{\mathrm{sup}} + V_d)^2} \qquad (23a)$$

$$= \frac{2\theta - \sin 2\theta}{\cos^2 \theta}. \qquad (23b)$$

Fig. 5 shows the maximum recycling efficiency achievable and the recycling factor as a function of the diode conduction angle. Hence, the maximum achievable recycling efficiency is related to the recycling factor—the circuit parameters of the recycling network—through the diode conduction angle. For example, it can be seen that for the recycling efficiency higher than 55%, the diode conduction angle must keep below $60°$, or correspondingly, the recycling factor must be chosen less than five. The diodes, power supply and the available power are then traded off according to (23). Also note an interesting result—the smaller the diode conduction angle, the more RF power is converted to dc and, hence, the higher the recycling efficiency. This reminds us of the fact that in classical power amplifier design, which can be considered as a dc-RF converter, the bias point of the transistor is lowered to reduce the transistor conduction angle and improve the drain efficiency. Fig. 6 shows the maximum recycling efficiency as a function of the recycling factor.

In practice, the impedance matching network is usually fixed and the available power to the recycling network varies with time, for example, in the case of linear modulated signals. The analysis shows that the maximum recycling efficiency in this case generally does not occur at the same point as the lowest VSWR. Following the similar procedures, it can be shown that the maximum recycling efficiency is given by:

$$\eta_{r,\max} = \frac{V_{\mathrm{sup}}}{V_{\mathrm{sup}} + V_d}$$

$$\cdot \frac{3\tan\theta + \theta(4\theta^2 \csc^2\theta - 4\theta\tan\theta + \sec^2\theta - 8)}{2\theta - 2\tan\theta}$$

$$(24a)$$

$$\approx \frac{3\tan\theta + \theta(4\theta^2 \csc^2\theta - 4\theta\tan\theta + \sec^2\theta - 8)}{2\theta - 2\tan\theta}.$$
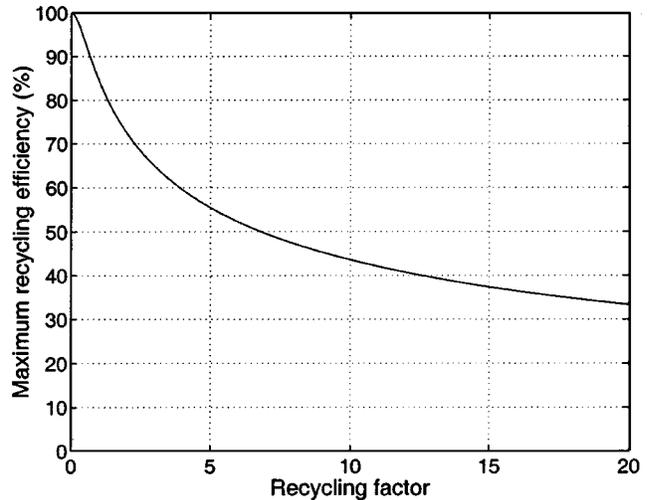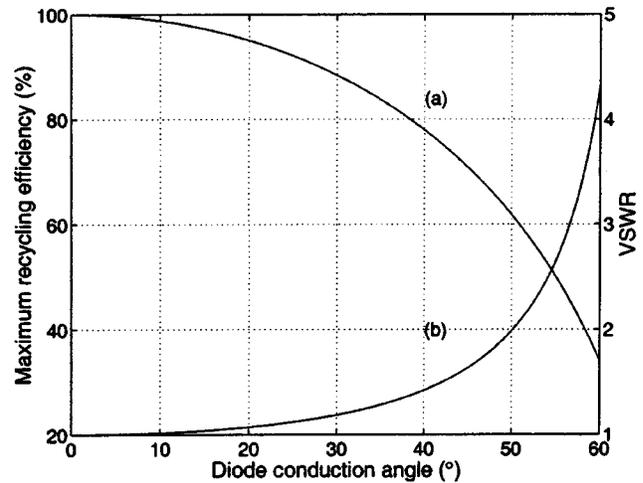
$$(24b)$$

Fig. 7. (a) Maximum recycling efficiency. (b) Correspondent VSWR as a function of the diode conduction angle.

And correspondingly, the input impedance of the recycling network under the optimum recycling efficiency is

$$Z_{\mathrm{in}} = Z_0 \frac{8\theta^2 + 4\theta\cos 2\theta\tan\theta + 3\cos 3\theta\sec\theta - 3}{2(\tan\theta - 2\theta)(2\theta - \sin 2\theta).} \qquad (25)$$

The diode conduction angle in above equations is determined by the following equation

$$\frac{Z_0}{n^2\pi R_d} = \frac{4\tan\theta - 8\theta}{8\theta^2 + 4\theta\cos 2\theta\tan\theta + 3\cos 3\theta\sec\theta - 3}. \qquad (26)$$

Note that the diode conduction angle and, hence, the maximum recycling efficiency is independent of the supply voltage. Equations (24) and (25) imply that the conditions for the maximum recycling efficiency and for the lowest VSWR are generally different. In practice, they are nevertheless fairly close to each other. This situation is illustrated in Fig. 7, in which the maximum recycling efficiency and the correspondent VSWR are plotted as a function of the diode conduction angle. Obviously, in most cases VSWR under the optimum efficiency is less than two, especially for the low diode conduction angle. This is in agreement with the experimental results by comparing [10, Figs. 1 and 2].
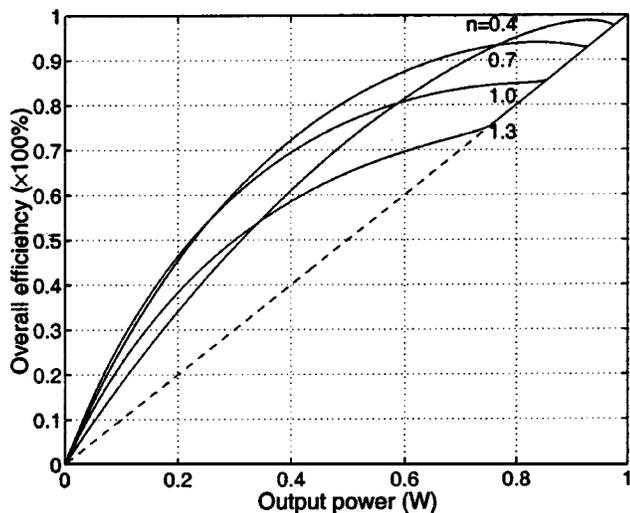
Fig. 8. Overall power efficiency as a function of the output power for different "n."

Fig. 9. VSWR as a function of the output power for different "n."

In practical applications, the losses of the critical components, such as hybrid splitter, isolator, and impedance transformation network should be minimized. In general, the splitter and isolator exhibit 0.5–1.0 dB insertion loss. Each 1-dB loss will degrade the recycling efficiency approximately by a factor of 20%.

IV. ANALYSIS AND DISCUSSION FOR A LINEAR MODULATED SIGNAL

For the linear modulations, the available power to the recycling network experiences a large variation while the total power delivered by the two power amplifiers is constant. The instantaneous overall efficiency η_o is rewritten here

$$\eta_o = \frac{p}{1 - (1-p)\eta_r} \qquad (27)$$

where p is the normalized output power of the amplifier system, equivalent to η_h in (18). Fig. 8 displays the overall power efficiency as a function of the output power for four different impedance transformation ratios. The dashed line corresponds to the case without power recycling, in which the power efficiency is equal to the normalized output power. With the power recycling, the overall power efficiency is enhanced. The solid lines show that the power efficiency improvement is dependent on the impedance matching network. The improvement near the low output power level is actually more critical than in the high output power level. The reason is that when the output power is high, little power goes to the recycling network and the overall power efficiency is high anyway. Note that each solid line overlaps with the dashed line above a certain power level, depending on the matching network. These intersection points correspond to where the diodes turns OFF, due to the fact that beyond these points less power is delivered to the recycling network and the voltage applied to the diodes is unable to overcome the power supply and turn on the diodes. The VSWR of the recycling network beyond these points is of course infinite, as shown in Fig. 9. Proper choice of the impedance matching network would result in a reasonably low VSWR ($<2:1$) across a wide range of the output power level.
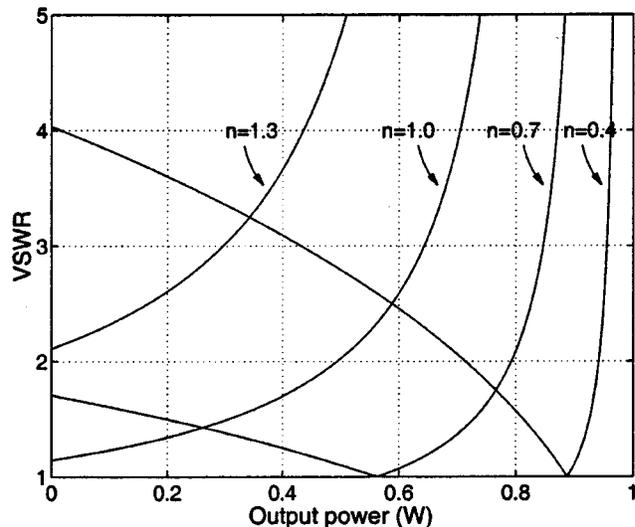
The average power efficiency for the linear modulated signal is calculated by integrating the instantaneous overall power efficiency weighted by the probability density over the output power, i.e.

$$\overline{\eta}_o = \int_0^1 \frac{p}{1 - (1-p)\eta_r(p)} \, \rho(p)dp \qquad (28)$$

where $\rho(p)$ is the power probability density function of the modulation. As can be seen from Fig. 8, the instantaneous overall power efficiency and, hence, the average power efficiency are strongly dependent on the impedance matching network. As two extreme cases, when the transformation ratio "n" of the impedance matching network tends to infinity, the voltage applied to the diodes unable to turn them ON most of the time, and the average power efficiency of the system is, hence, similar to the case without the power recycling. On the other hand, when the transformation ratio "n" tends to zero, the diodes are most often kept turned ON. In this case, the large signal impedance of the diodes approximates to zero, and most of the RF power delivered to the recycling network will be reflected back to the isolator, thus, the average power efficiency of the system is also low. Obviously, there exists an optimum impedance matching for the maximum average power efficiency, depending on the probability density of the modulated signal. A Mathematica program was written to determine this optimum point and the correspondent peak average power efficiency.

The probability density function of the modulated signal is required to calculate the power efficiency with and without the power recycling. The analytical expression of the probability density generally can not be found and, hence, the histogram from the simulation is used instead, as shown in Fig. 10. The modulations under investigation include QPSK, OQPSK, $\pi/4$-DQPSK, 16-QAM, and 64-QAM with square-root raised cosine filtering. The roll-off factor of the shaping filter varies from 0.1 to 1.0, with an increment of 0.1. Note that in practical applications, the signal in-phase and quadrature components may be offset by half the symbol period for 16-QAM and 64-QAM and the probability distribution will be different, as
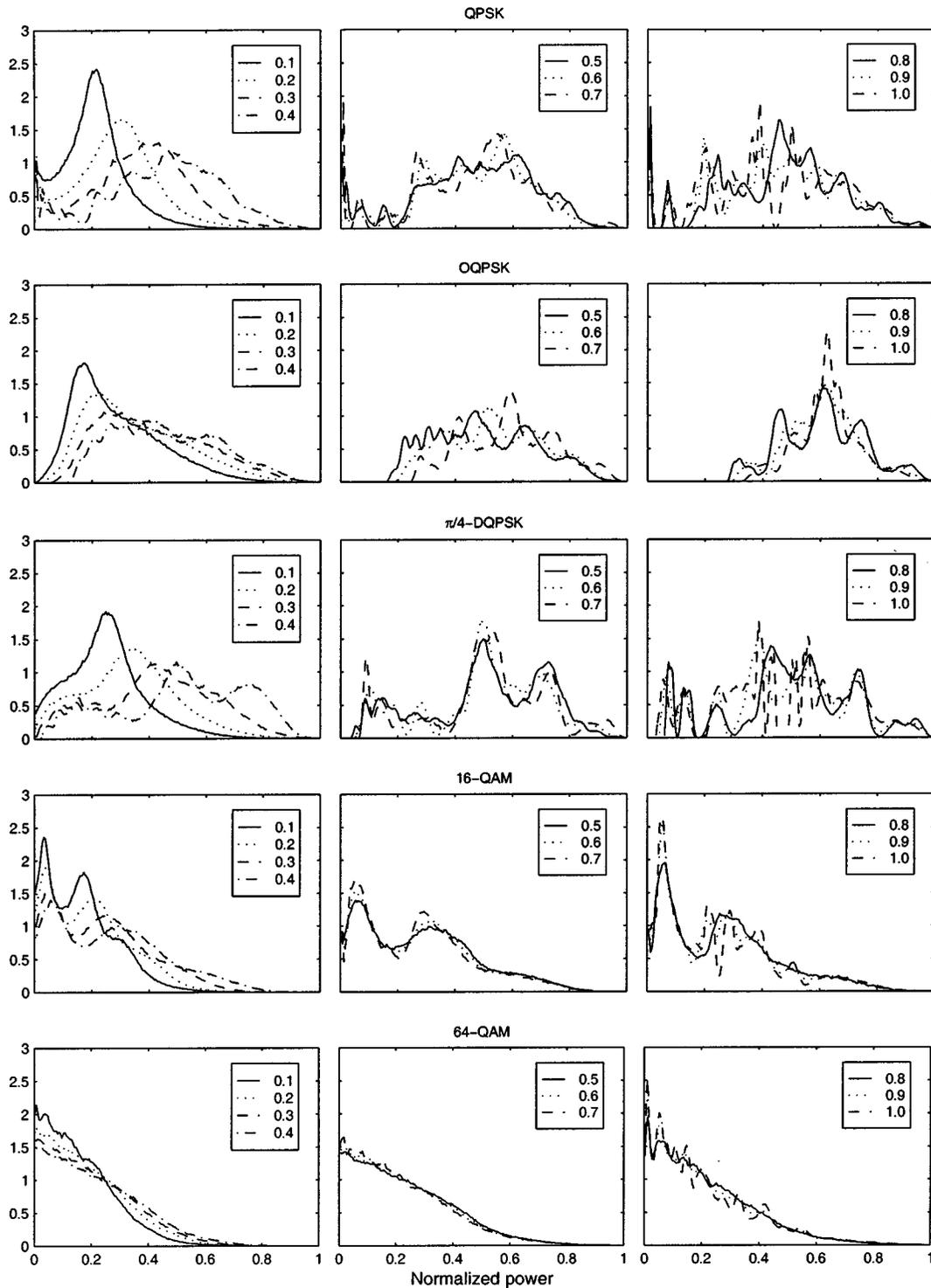
Fig. 10.   Power probability density function for various modulations. The legend indicates the roll-off factors of the square-root raised cosine filtering.

in the case of QPSK and OQPSK. In Fig. 11, the solid curves correspond to the calculated peak average power efficiency with the optimum impedance matching as a function of the roll-off factor for various modulations. The average power efficiency without the recycling network is also displayed as the dashed lines to show the improvement. In this calculation, the maximum output power of the amplifier system is 1 W. The supply voltage is 3 V and the diode on-resistance is 5 Ω. The recycling factor is, hence, 2.7, which corresponds to a

maximum 57% recycling efficiency for the full power level, and a maximum 65% recycling efficiency for the mid power level, according to (22) and (23). As illustrated in Fig. 11, with properly chosen impedance matching network, the net increase of the average power efficiency is between 14% and 21% throughout the entire range of roll-off factor ($\alpha = 0.1 \sim 1.0$), depending on the modulations. This corresponds to the relative improvement of the average power efficiency from 33% to 83%. Note that the probability density functions in this calculation
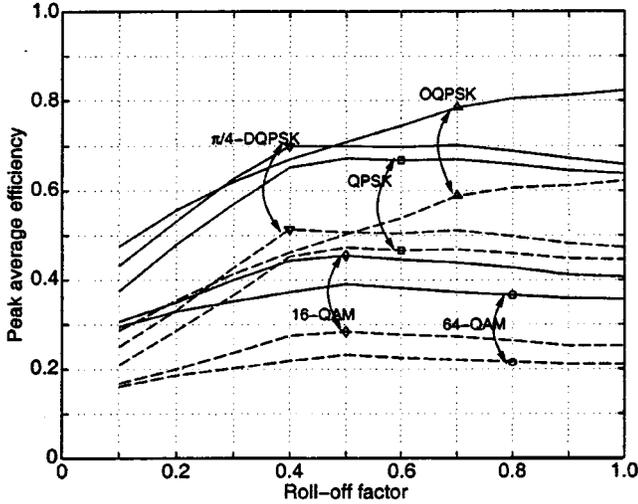
Fig. 11.   Average power efficiency with (solid lines) and without (dashed lines) the recycling network as a function of the roll-off factor for various modulations.

experience differing distributions, while the net increase of the average power efficiency is approximately 16% for 16-QAM and 64-QAM, and approximately 20% for QPSK, OQPSK, and $\pi/4$-DQPSK, except with the modest drop for the case of roll-off factor 0.1. As shown in Fig. 10, the probability density of the $\pi/4$-DQPSK modulated signal typically possesses one or two peaks in certain medium power levels and rolls off on both sides. The OQPSK modulated signal roughly approximates a constant envelope, hence, its probability density concentrates within a certain range of power levels well above dc. In the case of 64-QAM, the probability density function tends to be Gaussian and the peak-to-average power ratio is pretty low. In a word, the proper choice of R_d, V_{sup}, and P_{ava} is critical to the performance of the recycling network, and Fig. 5 can be a useful guidance for the estimation of the improvement.

For multicarrier channels in the basestation, the probability density function of the modulated carrier tends to be Gaussian distributed, according to the Central Limit Theorem. This will make the behavior of the recycling network much like in the high-level modulation case, such as 64-QAM. The bandwidth of the power recycling system is generally determined by the impedance matching network. As demonstrated in [10], a simple design of the impedance matching network made the system with sufficient bandwidth for CDMA IS-95 modulated signal.

It is essential to reduce the diode loss to maximize the system performance. The diode "on-resistance" can be reduced by parallel connection of a few diodes, but the shunt capacitance increases. The optimum design of the recycling network may be fine-tuned with SPICE simulation and the experiment. It is also important to properly choose the matching network to prevent high reverse voltage applied to the Schottky diodes for breakdown.

V. Conclusion

The power recycling technique has been analyzed for the optimum efficiency performance for the outphasing power amplifiers. The analysis demonstrates that the proper tradeoff among

the diodes, the power supply and the available power to the recycling network is critical for the performance of the system. The numerical calculations predict that a relative improvement of 33% to 83% on the average power efficiency can be achieved for various modulations. This simple technique promises to improve the power efficiency of the outphasing microwave power amplifier, while maintain its high linearity performance, and make it more attractive for mobile wireless communications.

Appendix
Recycling Efficiency and VSWR for an Arbitrary Diode Model

The voltage–current characteristic of a Schottky barrier is usually described by empirical equations. More generally, the following arbitrary current–voltage relationship of the Schottky diode is assumed

$$I_D = f(V_D) \tag{29}$$

where V_D is the voltage drop across to the diode. Then, the dc component of the diode current can be found

$$i_0 = \frac{1}{2\pi} \int_{-\pi}^{\pi} f\left(V_{\mathrm{pk}} \cos\phi - V_{\mathrm{sup}}\right) d\phi \tag{30}$$

and the fundamental component is

$$i_1 = \frac{1}{\pi} \int_{-\pi}^{\pi} f\left(V_{\mathrm{pk}} \cos\phi - V_{\mathrm{sup}}\right) \cos\phi \, d\phi. \tag{31}$$

The same expressions for the available power (15a) and the recycling efficiency (17) can also be obtained as a function of V_{pk}. The concept of diode conduction angle in this more general case is meaningless. The maximum recycling efficiency is determined by differentiating (17) with respect to the impedance transformation ratio "n" for the fixed available power to the recycling network. Similarly, (15a) can be regarded as the implicit function of "n" and V_{pk}. Finally, we have

$$\frac{d\eta_r}{dn} = \frac{2V_{\mathrm{sup}}}{P_{\mathrm{ava}}} \frac{di}{dV_{\mathrm{pk}}} \frac{dV_{\mathrm{pk}}}{dn} \tag{32a}$$

$$= \frac{4V_{\mathrm{pk}}}{P_{\mathrm{ava}}} \frac{\int_{-\pi}^{\pi} f'(V_{\mathrm{pk}} \cos\phi - V_{\mathrm{sup}}) \cos\phi \, d\phi}{n\pi + \frac{Z_0}{n} \int_{-\pi}^{\pi} f'(V_{\mathrm{pk}} \cos\phi - V_{\mathrm{sup}}) \cos^2\phi \, d\phi}$$

$$\cdot \left(\frac{Z_0}{n^2} i_1 - V_{\mathrm{pk}}\right). \tag{32b}$$

The maximum recycling efficiency occurs as the above expression is equal to zero, which is equivalent to

$$Z_0 = n^2 \frac{V_{\mathrm{pk}}}{i_1} \tag{33a}$$

$$= Z_{\mathrm{in}}. \tag{33b}$$

Equation (33) concludes that in the case of the fixed available power to the recycling network, the maximum recycling efficiency and the lowest VSWR occur simultaneously. This conclusion is general and independent of the diode model, which is a direct consequence of the maximum power transfer theorem.

REFERENCES

[1] H. Chireix, "High power outphasing modulation," *Proc. IRE*, vol. 23, pp. 1370–1392, Nov. 1935.

[2] D. C. Cox, "Linear amplification with nonlinear components," *IEEE Trans. Commun.*, vol. COM-23, pp. 1942–1945, Dec. 1974.

[3] L. Couch and J. L. Walker, "A VHF LINC amplifier," in *Proc. IEEE Southeastcon*, Destin, FL, April 4–7, 1982, pp. 122–125.

[4] S. A. Hetzel, A. Bateman, and J. P. McGeehan, "LINC transmitter," *Elecron Lett.*, vol. 27, no. 10, pp. 844–846, May 9, 1991.

[5] F. H. Raab, "Efficiency of outphasing RF power-amplifier systems," *IEEE Trans. Commun.*, vol. COM-33, pp. 1094–1099, Oct. 1985.

[6] C. P. Conradi, R. H. Johnston, and J. G. McRory, "Evaluation of a lossless combiner in a LINC transmitter," in *Proc. IEEE Canadian Conf. Electrical and Computer Engineering*, Edmonton, AB, Canada, May 1999, pp. 105–110.

[7] B. Stengel and W. R. Eisenstadt, "LINC power amplifier combiner method efficiency optimization," *IEEE Trans. Veh. Technol.*, vol. 49, pp. 229–234, Jan. 2000.

[8] L. Sundstrom and M. Johansson, "Effect of modulation scheme on LINC transmitter power efficiency," *Electron. Lett.*, vol. 30, no. 20, pp. 1643–1645, Sept. 29, 1994.

[9] L. Sundstrom, "The effect of quantization in a digital signal component separator for LINC transmitters," *IEEE Trans. Veh. Technol.*, vol. 45, pp. 346–352, May 1996.

[10] R. Langridge, T. Thornton, P. M. Asbeck, and L. E. Larson, "A power re-use technique for improved efficiency of outphasing microwave power amplifiers," *IEEE Trans. Microwave Theory Technol.*, vol. 47, pp. 1467–1470, Aug. 1999.

[11] S. C. Cripps, *RF Power Amplifiers for Wireless Communications*. Norwood, MA: Artech House, 1999.

Xuejun Zhang received the B.S. degree in semiconductor physics from Peking University, Beijing, China in 1991 and the M.S. degree in electrooptics from the National University of Singapore, Singapore, in 1997. He received the Ph.D. degree in electrical engineering from the University of California, San Diego, in 2001.

From 1991 to 1992, he was with Southwestern Computing Center, China. From 1992 to 1995, he was with the Institute of Applied Electronics, China, where he was involved in various research projects, including laser optics, optical diagnostic system, nonlinear optics, and optical materials. Currently, he is a Senior RF Engineer at Qualcomm, Inc., San Diego, CA, where he is involved in circuit design and research on RF frond-end for wireless communications.

Lawrence E. Larson (S'83–M'86–SM'90–F'00) received the B.S. degree in electrical engineering and the M.Eng. degree from Cornell University, Ithaca, NY, in 1979 and 1980, respectively, and the Ph.D. degree in electrical engineering from the University of California, Los Angeles, in 1986.

In 1980, he joined Hughes Research Laboratories, Malibu, CA, where he directed work on high-frequency InP–GaAs, and silicon integrated circuit development for a variety of radar and communications applications, as well as MEMS-based circuits for RF and microwave applications. From 1992 to 1994, he was Assistant Program Manager of the Hughes/DARPA MIMIC Program. From 1994 to 1996, he was with Hughes Network Systems, Germantown, MD, where he directed the development of radio-frequency integrated circuits for wireless communications applications. In 1996, he joined the faculty at the University of California, San Diego (UCSD), La Jolla, where he is the Inaugural Holder of the Communications Industry Chair. Currently, he is the Director of the UCSD Center for Wireless Communications. He has published more than 150 papers and has received 25 U.S. patents.

Dr. Larson is a Member of Sigma Xi and Eta Kappa Nu. He was a corecipient of the 1996 Lawrence A. Hyland Patent Award of Hughes Electronics for his work on low-noise millimeter-wave HEMTs, and the 1999 IBM Microelectronics Excellence Award for his work on the development of Si/SiGe HBTs.

Peter M. Asbeck (M'75–SM'97–F'00) received the B.S. and Ph.D. degrees from the Electrical Engineering Department, Massachusetts Institute of Technology (MIT), Cambridge, in 1969 and 1975, respectively.

He was with Sarnoff Research Center, Princeton, NJ, and at Philips Laboratory, Briarcliff Manor, NY, working in the areas of quantum electronics and GaAlAs–GaAs laser physics and applications. In 1978, he joined Rockwell International Science Center, where he was involved in the development of high-speed devices and circuits based on III–V compounds and heterojunctions. He pioneered the effort to develop heterojunction bipolar transistors based on GaAlAs–GaAs and InAlAs–InGaAs materials, and has contributed widely in the areas of physics, fabrication, and applications of these devices. In 1991, he became a Professor in the Department of Electrical and Computer Engineering, University of California, San Diego. His research interests are in the development of high-speed heterojunction transistors and optoelectronic devices, and their circuit applications. He has written more than 220 publications.

Dr. Asbeck is a Distinguished Lecturer of the IEEE Electron Devices Society and of the Microwave Theory and Techniques Society. He was the General Chairman of the 1996 Device Research Conference, and of the 1999 IEEE Topical Workshop on Power Amplifiers for Wireless Communications.

Robert A. Langridge (S'83–M'86) received the B.S.E.E. degree from Iowa State University, Ames, in 1986 and the M.S.E.E. degree from the University of California, San Diego, La Jolla, in 1999.

From 1986 to 1987, he was with Boeing Military Airplane Company, Wichita, KS, where he was involved with digital and RF circuit design and analysis. From 1987 to 1993, he was with IFR Systems Inc., Wichita, KS, where he worked on several RF and analog design projects related to communication service monitors and general-purpose spectrum analyzers, including an RF signal generator, various frequency synthesizer projects, and spectrum analyzer IF design. From 1993 to 1994, he was with Sciteq Electronics Inc., San Diego, CA, where his work included phase-locked loop frequency synthesizers for various applications, which included fractional-N techniques. From 1995 to 1997, he was with Glenayre Electronics Inc., Quincy, IL, where he was involved in the RF front-end design of high-dynamic-range low-noise receivers for 900-MHz two-way paging systems. Currently, he is a Senior RF Engineer at Rockwell Collins, Cedar Rapids, IA, where he is involved in circuit design and research of front-end circuitry for communications receivers, systems analysis of receivers and exciters, and applications of MEMS device technology. He holds one patent.

Mr. Langridge is a Member of Eta Kappa Nu.